Available online at www.sciencedirect.com

ScienceDirect

Procedia CIRP 53 (2016) 252 – 260

www.elsevier.com/locate/procedia

The 10th International Conference on Axiomatic Design, ICAD 2016

Axiomatic design method for the hydrostatic spindle with multisource coupled information

QianJia[a,b], BinLi[a,b], YangyangWei[a], YaolongChen[b], JianleiWang[c], XiaoyangYuan[a,*]

[a]*Key Laboratory of Education Ministry forModern Design and Rotor-BearingSystem, Xi'an Jiaotong University, Xi'an, 710049, PR China*

[b]*State Key Laboratory for Manufacturing Systems Engineering, Xi'an Jiaotong University, Xi'an, 710049, PR China*

[c]*Schoolof Mechanical and Precision Instrument Engineering, Xi'an University of Technology, Xi'an 710048, PR China*

* Corresponding author. Tel.: +8629-8266-9152; fax: +8629-8266-9152.*E-mail address:* xyyuan@mail.xjtu.edu.cn

Abstract

The strong coupling among different parts such as bearings, seals, and windings, which are associated with different fields such as tribology, dynamics, and fluid dynamics, should be addressed to design a high-performance hydrostatic spindle. For decoupling and integrating all multisource information, the axiomatic design is using to address the design problems. A mapping with four levels of functional requirements and design parameters (DPs) was developed for the hydrostatic spindle design, and 19 DPs for the physical parts of the hydrostatic motorized spindle were integrated in several parts such as rotor, bearing, and winding. A 19×19 design matrix was built. Using the design matrix, a flow chart for the dynamics design method coupled with multisource information was obtained. The design of a hydrostatic spindle was completed, and the major requirements were assessed. The results show that the dynamics design process and hydrostatic spindle can be optimized using the axiomatic design method.

Peer-review under responsibility of the scientific committee of The 10th International Conference on Axiomatic Design

Keywords: axiomatic design; hydrostatic spindle; multisource Information

1. Introduction

Spindle is the core component of numerically controlled machine tools. With the rapid development of high-end manufacturing, the requirements of a spindle have increased [1]. Generally, a spindle is composed of bearings, seals, rotors, and other components such as stator and coil. A spindle supported with hydrostatic bearings is called a hydrostatic spindle [2]. As a typical kind of rotating equipment, the conceptual design phase of a hydrostatic spindle is very important, because of the performance requirements of hydrostatic spindle such as a high precision, high speed, and high stability [3].The design of a spindle is a complex process, it requires knowledge from different disciplines such as tribology, dynamics, and fluid mechanics.

The design of a hydrostatic spindle should first follow a general design principle that satisfies the requirements of the application. In terms of previous works, the vibration characteristics of a high-speed spindle type GDH512 were studied by Liangsheng Wu[4].The high precision of shafting was analyzed by Xianxin Zhong using the dimension chain theory [5].A high-speed spindle was studied by Bo Wang; during the high-speed operation of the spindle, bearing radial stiffness, centrifugal force, and gyroscopic effects significantly affected the dynamic characteristics of the spindle system[6].Most of the spindle designs were completed based on the designers' experience, without a systemic theoretical guidance [7]. In the past, however, the multifield and multipart coupling in spindle design has been rarely studied. In this study, the Axiomatic Design theory is employed to address such an issue. This involves the coupling of multisource information obtained from multicomponents and multiphysics fields and multidisciplines.

The axiomatic design is a set of mature design theory; it was proposed by SUH [8–10]. To achieve this design, strategies using the Axiomatic Design and Design-Centric Complexity theories were introduced to guide the creation and improvement of complex time-independent and time-

Peer-review under responsibility of the scientific committee of The 10th International Conference on Axiomatic Design
doi:10.1016/j.procir.2016.07.013

dependent technical systems [11]. In the design and operation of engineering systems such as products and manufacturing systems, the goal is to reduce complexity [12]. The axiomatic design theory has certain advantages in the design domain such as the identification of functional coupling degree, quantification of coupling degree, and decoupling. The axiomatic design theory has been applied well to the design of complex systems with multiple components and process design. Ananthkris-Hnan developed an aircraft coupling control system based on axiomatic design, thus simplifying complex control systems [11–13]. Qian Jia used the axiomatic design theory in studying the Babbitt metal-forming process for a high-speed spindle sliding bearing [14]. This research is based on a large number of studies on the performance of the bearing, seal, rotor, and other components of a hydrostatic spindle system. In this study, the axiomatic design theory was used as a guide for a detailed and specific hydrostatic spindle design to make full use of the advantages of the proposed design method, transform the traditional rotor system design from coupled dispersed to integration, and improve the efficiency and quality of the design.

2. Design principles of a hydrostatic spindle require multisource information

A hydrostatic spindle is designed to satisfy the requirements of an application. The design of a hydrostatic spindle involves the selection of a torque motor and rotary encoder, as well as the design of the cooling, sealing, and hydraulic systems. A hydrostatic spindle typically contains two radial bearings and two thrust bearings, and the spindle has sufficient radial and axial stiffness, but these increase the difficulty of machining and assembly. There are two types of torque motor: built-in and external. The motor volume of a built-in torque is small, and its installation is easy. The motor volume of an external rotor torque is high, but it can provide a high driving force. The selection of a rotary encoder depends on the application-required accuracy including the position and speed control accuracy. The position accuracy is the highest performance influenced by an encoder on a motor.

The heat of a hydrostatic spindle mainly originates from the motor and bearing. The temperature of a spindle increases if the heat cannot be discharged effectively. Then, the machining accuracy is affected. Therefore, a cooling system should be designed properly. Lubricating oil is the working medium of a spindle; all the oil lines should be sealed. Seal is divided into static and dynamic seal. Static seal occurs between two relatively static parts. Dynamic seal occurs between two relatively rotating parts. In different applications, dynamic seals are divided into pneumatic, labyrinth, centrifugal, magnetic, and spiral seals. The performance of a spindle depends on the hydraulic station. A hydraulic station design must satisfy the following conditions: (1) The pressure and flow satisfy the requirements of hydrostatic bearing design, (2) the lubricating oil does not contain impurities, (3) a safety protection device should be present, and (4) the hydraulic station should have a sufficient heat dissipation area or a thermostat.

The design criteria of a hydrostatic spindle are shown in Table 1, including radial motion error, axial motion error, positioning precision, repetitive positioning accuracy, radial stiffness, axial stiffness, and design speed. The design was mainly evaluated as follows: (1) Measure the motion error. The motion rotation errors including radial and axial motion errors significantly affect the processing precision. (2) Measure the static stiffness. During a high-speed operation, if the static stiffness of the spindle is low, the machining accuracy is affected. Spindle static stiffness test is the most direct and effective method to obtain the static stiffness. (3) Measure the speed. The speed of a spindle significantly affects the cutting force; it determines the machining precision.

Table 1.Design criteria of hydrostatic spindle

Name of indicators	Definition of indicators
Radial motion error	Radial drift from the ideal rotation axis
Axial motion error	Axial drift from the ideal rotation axis
Positioning accuracy	Accuracy the location of the machine moving parts movement can achieve
Repeat positioning accuracy	Precision of laser interferometer detection when spindle reciprocating motion fivetimes in 360°
Radial stiffness	Radial force resistance to elastic deformation
Axial stiffness	Axial force resistance to elastic deformation
Design speed	Turn number per minute of the spindle rotor

3. Decomposition of functional requirements (FRs) and mapping of design parameters (DPs)

3.1. First-layer decomposition of FRs decomposition and mapping of DPs

According to axiomatic design, the FRs should be considered first when designing a hydrostatic spindle. The FRs and DPs should be established. The total FR is shown in Fig. 1.The first layer of FR decomposition and DP mapping is shown in Table 2. Eq. (1) shows the design equations. The design matrix is a triangular matrix; this shows that the design is decoupled. In the design equation of axiomatic design, X represents the relationship between the FRs and DPs. These relationships constitute the design matrix. If the matrix is a diagonal matrix, the design is an uncoupled design; if the matrix is a triangular matrix, the design is a coupling design.

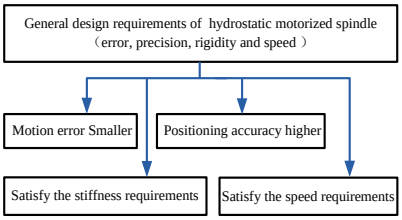

Fig. 1. Requirements of design functional for the spindle

$$\begin{pmatrix} FR_1 \\ FR_2 \\ FR_3 \\ FR_4 \end{pmatrix} = \begin{pmatrix} X & 0 & 0 & 0 \\ 0 & X & 0 & 0 \\ 0 & 0 & X & 0 \\ 0 & 0 & 0 & X \end{pmatrix} \begin{pmatrix} DP_1 \\ DP_2 \\ DP_3 \\ DP_4 \end{pmatrix} \quad (1)$$

Design matrixes show the coupling relationship only, 0 indicates no coupling between the FRs and DPs.

Table 2. Functional decomposition and parameter mapping of the first layer

FR domain	Functional escription	DP domain	Parametric description
FR_1	Satisfy the error requirements	DP_{111}	Kinematic error
FR_2	Satisfy the accuracy requirements	DP_{112}	Positioning/Repeat positioning accuracy
FR_3	Satisfy the stiffness requirements	DP_{113}	Spindle rigidity
FR_4	Satisfy the speed requirements	DP_{112}	Rated speed

3.2. Second-layer decomposition of FRs and mapping of DPs

Considering the DPs on the first layer, the second layer satisfies their requirement. The decomposition affords the DPs according to the FR. The motion error DP_1 and positioning/repeat positioning accuracy DP_2 are the main problems that should be considered in a spindle design. The spindle rigidity DP_3 and rated speed DP_4 are the required guarantee for a running spindle; they should achieve certain requirements or standards. This is a requirement for structure design and parameter calculation, because the choke can reach a certain rigidity. If an appropriate torque motor is selected, the spindle can reach a certain speed. The second FR decomposition and DP mapping are shown in Table 3.

Table 3. Functional decomposition and parameter mapping of the second layer

FR domain	Functional description	DP domain	Parametric description
FR_{11}	Improve the rotary accuracy	DP_{11}	Related factors that affect the rotation accuracy
FR_{12}	Determine the structural parameters	DP_{12}	Mathematical modeling for the shafting
FR_{21}	Improve the positioning accuracy	DP_{21}	Select the appropriate rotary encoder
FR_{22}	Improve the repeat positioning accuracy	DP_{22}	Select the appropriate feedback control
FR_{31}	Achieve a high stiffness	DP_{31}	Calculation for the spindle rigidity
FR_{32}	Determine the structural parameters	DP_{32}	Calculation for the structure of the choke
FR_{41}	Satisfy the design speed	DP_{41}	Select anappropriate torque motor
FR_{42}	Operation speed, avoid critical speed	DP_{42}	Eigen values for motion equations

The equation for the design of second layer is

$$\begin{cases} \begin{pmatrix} FR_{11} \\ FR_{12} \end{pmatrix} = \begin{pmatrix} X & 0 \\ 0 & X \end{pmatrix} \begin{pmatrix} DP_{11} \\ DP_{12} \end{pmatrix} \\ \begin{pmatrix} FR_{21} \\ FR_{22} \end{pmatrix} = \begin{pmatrix} X & 0 \\ X & X \end{pmatrix} \begin{pmatrix} DP_{21} \\ DP_{22} \end{pmatrix} \\ \begin{pmatrix} FR_{31} \\ FR_{32} \end{pmatrix} = \begin{pmatrix} X & 0 \\ 0 & X \end{pmatrix} \begin{pmatrix} DP_{31} \\ DP_{32} \end{pmatrix} \\ \begin{pmatrix} FR_{41} \\ FR_{42} \end{pmatrix} = \begin{pmatrix} X & 0 \\ X & X \end{pmatrix} \begin{pmatrix} DP_{41} \\ DP_{42} \end{pmatrix} \end{cases} \quad (2)$$

3.3. Third-layer decomposition of FRs and mapping of DPs

3.3.1 Decomposition of FR_{11} and mapping of DPs

The factors to improve rotary precision DP_{11}were evaluated. The kinematic characteristics of the decision support components decide the rotation accuracy. In a motorized spindle system, the supporting elements of the movement characteristics of several main factors are as follows: (1) Radial sliding bearing. Sliding bearing is the main factor for the instability of a shaft system; its dynamic performance is characterized by four stiffness and four damping coefficients. If the tangential force is higher than the damping force, the shafts become unstable. (2)Seal. The presence of a seal provides a vertical force for the shafts. This force is always applied along the tangent of the vortex trajectory, leading to the instability of the system. Similar to sliding bearing, the dynamic performance of a seal can also be characterized using four linear stiffness coefficients. (3)Thrust bearing. The stiffness along the axial direction can be attributed to thrust bearing. When the rotor is equipped with a tilt, the torque acts along the axial direction.

A motorized spindle system uses two static-pressure sliding bearing; its movement characteristics can be improved using the following measures: (1)use a static pressure bearing for a better stability, (2)optimize the rigidity of components including the sealing, (3)select an appropriate oil pressure for the hydraulic system, and (4)reduce the effect of winding. The third FR decomposition and DP mapping are shown in Table 4.

Table 4. Functional decomposition and parameter mapping of the third floorFR11

FR domain	Functional description	DP domain	Parametric description
FR_{111}	Improve the kinematics performance of sliding bearing	DP_{111}	Using hydrostatic bearing and optimization of the stiffness of bearing
FR_{112}	Improve the kinematics performance of other supporting components	DP_{112}	Optimization of the stiffness of supporting components
FR_{113}	Improve the working conditions	DP_{113}	Select an appropriate pressure for hydraulic oil supply
FR_{114}	Reduce the influence from other components	DP_{114}	Reduce the influence from winding

Eq. (3) shows the design equations. The design matrix is a diagonal matrix; therefore, it is an uncoupled design.

$$\begin{pmatrix} FR_{111} \\ FR_{112} \\ FR_{113} \\ FR_{114} \end{pmatrix} = \begin{pmatrix} X & 0 & 0 & 0 \\ 0 & X & 0 & 0 \\ 0 & 0 & X & 0 \\ 0 & 0 & 0 & X \end{pmatrix} \begin{pmatrix} DP_{111} \\ DP_{112} \\ DP_{113} \\ DP_{114} \end{pmatrix} \quad (3)$$

3.3.2 Decomposition of FR_{12} and DP mapping

For a mathematical model of rotor-bearing system DP_{12}, a simple sliding bearing rotor system was used at the ends of the rotating shaft using a spring support. This model explained the problem qualitatively, but not precise enough.

The complex bearing rotor system in this study was used to obtain the dynamic characteristics of the spindle. For this purpose, a calculation model was established. The following three aspects were considered for the development of a reasonable computing model: (1) the structure of a system and application conditions, (2) the analysis of mechanical problems, and (3) the existing calculation methods and calculation tools.

Because of the improvement in calculation methods and a rapid increase in computer speed, Riccati transfer-matrix, transfer-matrix impedance coupling, transfer-matrix-modal synthesis, and transfer-matrix-direct integral methods were developed. Several commercial software sets were developed based on the finite-element method using ANSYS.

The analysis of simple discrete rotor systems is mostly based on the analysis of the theoretical mechanics. The complex rotor system is a multipurpose transfer-matrix method and finite-element method as shown in this paper. The FR_{12} decomposition and DP mapping are shown in Table 5.

Table 5. Functional decomposition and parameter mapping of the third-layer FR_{12}

FR domain	Functional description	DP domain	Parametric description
FR_{121}	Establish a simplified model for shafting	DP_{121}	Using the single-massrigid rotor-disk model
FR_{122}	Establish a complex model for shafting	DP_{122}	Using transfer matrix method

The design matrix shown in Eq. (4) is a diagonal matrix; therefore, it is an uncoupled design.

$$\begin{pmatrix} FR_{121} \\ FR_{122} \end{pmatrix} = \begin{pmatrix} X & 0 \\ 0 & X \end{pmatrix} \begin{pmatrix} DP_{121} \\ DP_{122} \end{pmatrix} \quad (4)$$

3.3.3Decomposition of $FR_{31}$and its mapping DPs

For the calculation of spindle rigidity DP_{31}, the bearing-lubricating and film-rotor models were setup. The spindle system was first abstracted, and then the dynamic characteristics of the motorized spindle system were obtained. Finally, the spindle stiffness was calculated. The FR decomposition and DP mapping are shown in Table 6. The design matrix shown in Eq. (5) is a diagonal matrix; therefore, it is an uncoupled design.

Table 6. Functional decomposition and parameter mapping of the third-layer FR_{31}

FR domain	Functional description	DP domain	Parametric description
FR_{311}	Establish a model for bearing-lubricating and film-rotor	DP_{311}	Model based on Lubrication theory and fluid mechanics
FR_{312}	Calculate the rotor dynamic performance	DP_{312}	Rotor stiffness calculation

$$\begin{pmatrix} FR_{311} \\ FR_{312} \end{pmatrix} = \begin{pmatrix} X & 0 \\ 0 & X \end{pmatrix} \begin{pmatrix} DP_{311} \\ DP_{312} \end{pmatrix} \quad (5)$$

For the calculations of the structural parameters of the choke, first the type of choke was determined, and then the choke model was set up. The calculation of choke performance was mainly based on the aperture-pressure calculation. The FR decomposition and DP mapping are shown in Table 7.

Table 7. Functional decomposition and parameter mapping of the third-layer FR_{32}

FR domain	Functional description	DP domain	Parametric description
FR_{321}	Establish a model for the choke	DP_{321}	Small hole throttle model
FR_{322}	Calculate the performance for the choke	DP_{322}	Rotor stiffness calculation

The design matrix shown in Eq. (6) is a diagonal matrix; therefore, it is an uncoupled design.

$$\begin{pmatrix} FR_{321} \\ FR_{322} \end{pmatrix} = \begin{pmatrix} X & 0 \\ 0 & X \end{pmatrix} \begin{pmatrix} DP_{321} \\ DP_{322} \end{pmatrix} \quad (6)$$

For the Eigen values of the equations of motion DP_{42}, the FR decomposition and DP mapping are shown in Table8. The design matrix shown in Eq. (7) is a diagonal matrix; therefore, it is an uncoupled design.

Table 8. Functional decomposition and parameter mapping of the third-layer FR_{42}

FR domain	Functional description	DP domain	Parametric description
FR_{421}	Determine the dynamic parameters of bearing	DP_{421}	Stiffness and damping of bearing
FR_{422}	Dynamics analysis under the simplified model	DP_{422}	Based on dynamics equations
FR_{423}	Dynamics analysis under the rigid support	DP_{423}	Based on dynamics differential equations
FR_{424}	Dynamics analysis under the elastic support	DP_{424}	Based on equivalent mass solution
FR_{425}	Dynamics analysis of damping system	DP_{425}	Solving the differential equation of system dynamics in coupling conditions

$$\begin{pmatrix} FR_{421} \\ FR_{422} \\ FR_{423} \\ FR_{424} \\ FR_{425} \end{pmatrix} = \begin{pmatrix} X & 0 & 0 & 0 & 0 \\ X & X & 0 & 0 & 0 \\ X & 0 & X & 0 & 0 \\ X & 0 & 0 & X & 0 \\ X & 0 & 0 & 0 & X \end{pmatrix} \begin{pmatrix} DP_{421} \\ DP_{422} \\ DP_{423} \\ DP_{424} \\ DP_{425} \end{pmatrix} \quad (7)$$

To reduce the influence of winding DP_{114}, the FR decomposition and DP mapping are shown in Table9. The

design matrix shown in Eq. (8) is a diagonal matrix; therefore, it is an uncoupled design.

Table 9. Functional decomposition and parameter mapping of the fourth-layer FR_{114}

FR domain	Functional description	DP domain	Parametric description
FR_{1141}	The coil winding method	DP_{1141}	Calculation of electromagnetic torque
FR_{1142}	The coil number of turns	DP_{1142}	Calculation to strengthen the magnetic field

$$\begin{pmatrix} FR_{1141} \\ FR_{1142} \end{pmatrix} = \begin{pmatrix} X & 0 \\ 0 & X \end{pmatrix} \begin{pmatrix} DP_{1141} \\ DP_{1142} \end{pmatrix} \quad (8)$$

4. System structural characterization and design matrix of spindle

The hierarchical structure of the hydrostatic spindle design is shown in Fig. 2.

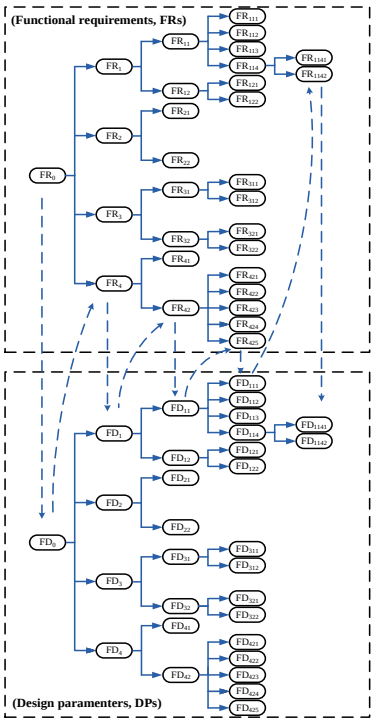

Fig. 2. Hierarchical structure for the FR and DP of the spindle

The design satisfied the FRs as determined from the design of each component. Those are the DPs of each layer. Therefore, a final design matrix was established. The matrix was used to describe the entire design outcome of all the DPs and FRs. This is according to different levels of the design matrix of FRs and the relationships with the DPs. The decomposition results for the spindle show 19 DPs, corresponding to 19 FRs. The final 19×19 design matrix describes the relationship between the DPs and FRs. According to the hierarchical structure of the design, the leaf DPs and the relationship between various FRs are listed in Table 10.

The spindle of the axiomatic design software module node structure, as shown in Fig. 2, can be obtained through the analysis of Table 7. As shown in Fig. 3, S represents no coupling between modules; the order is not considered in the process. C represents the decoupling relationship between the modules. Mi is defined as the design matrix of line; when a DP was input, the corresponding FR was obtained. Mi can be represented as formula (9).

$$M_i = \sum_{j=i}^{j=i} \frac{\partial FR_i}{\partial DP_j} \frac{DP_j}{DP_i} \quad (9)$$

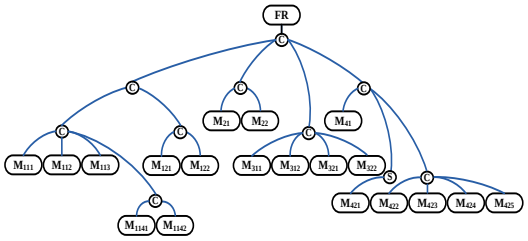

Fig. 3. Module node structure of the axiomatic design software for the hydrostatic spindle

Using the node properties, the module connection structure can be easily converted into a flow chart, and the flow chart shows the execution module and the data flow between. Fig. 4 shows the flow chart that describes the order of the hydrostatic spindle designs.

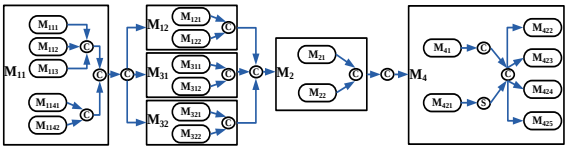

Fig. 4. Flow chart of the sequence for hydrostatic spindle design

Therefore, $M_{11}$is the design module to improve the rotary precision, M_{12} is the mathematical modeling module for the rotor-bearing system, M_{31} is the numeration module for the spindle rigidity, M_{32} is the numeration module for the structural parameters of the restrictor, $M_2$is the design module to improve the positioning accuracy, and $M_4$is the design module for the spindle speed. The process variables in the domain can be identified when the DPs are selected. The code

Table 10. Overall design matrix of the hydrostatic spindle

The domain of DPs	The domain of DPs																		
	DP_{111}	DP_{112}	DP_{113}	DP_{1141}	DP_{1142}	DP_{121}	DP_{122}	DP_{21}	DP_{22}	DP_{311}	DP_{312}	DP_{321}	DP_{322}	DR_{41}	DR_{421}	DR_{422}	DR_{423}	DR_{424}	DR_{425}
FR_{111}	X	0	0	0	0	0	0	0	0	0	0	0	0	0	0	0	0	0	0
FR_{112}	0	X	0	0	0	0	0	0	0	0	0	0	0	0	0	0	0	0	0
FR_{113}	0	0	X	0	0	0	0	0	0	0	0	0	0	0	0	0	0	0	0
FR_{1141}	0	0	0	X		0	0	0	0	0	0	0	0	0	0	0	0	0	0
FR_{1142}	0	0	0	0	X	0	0	0	0	0	0	0	0	0	0	0	0	0	0
FR_{121}	0	0	0	0	0	X	0	0	0	0	0	0	0	0	0	0	0	0	0
FR_{122}	0	0	0	0	0	0	X	0	0	0	0	0	0	0	0	0	0	0	0
FR_{21}	0	0	0	0	0	0	0	X	0	0	0	0	0	0	0	0	0	0	0
FR_{22}	0	0	0	0	0	0	0	X	X	0	0	0	0	0	0	0	0	0	0
FR_{311}	0	0	0	0	0	0	0	0	0	X	0	0	0	0	0	0	0	0	0
FR_{312}	0	0	0	0	0	0	0	0	0	0	X	0	0	0	0	0	0	0	0
FR_{321}	0	0	0	0	0	0	0	0	0	0	0	X	0	0	0	0	0	0	0
FR_{322}	0	0	0	0	0	0	0	0	0	0	X	0	X	0	0	0	0	0	0
FR_{41}	0	0	0	0	0	0	0	0	0	0	0	0	0	X	0	0	0	0	00
FR_{421}	0	0	0	0	0	0	0	0	0	0	X	0	0	0	X	0	0	0	0
FR_{422}	0	0	0	0	0	0	0	0	0	0	0	0	0	0	X	X	0	0	0
FR_{423}	0	0	0	0	0	0	0	0	0	0	0	0	0	0	X	0	X	0	0
FR_{424}	0	0	0	0	0	0	0	0	0	0	0	0	0	0	X	0	0	X	0
FR_{425}	0	0	0	0	0	0	0	0	0	0	0	0	0	0	X	0	0	0	X

for each module was written after the completion of the system architecture using the axiomatic design software. Then, these modules were combined into the main module to obtain the final results. In this paper, the modeling and performance simulation calculation of each module were performed using the SOLIDWORKS and MATLAB software, respectively.

5. Design example

The DPs of a spindle are listed in Table 11. Design ideas were proposed for the coupled design method developed in this study. For the shafting design of a concrete structure, the design of the supporting system, motor torque, cooling system, sealing system, and hydraulic system, selection of rotary encoder, and other key issues were considered. The main design process and measured indicators are described as follows:

Table 11. Design requirement for hydrostatic spindle

Name of indicators	Value of indicators
Radial motion error	0.3 μm
Axial motion error	0.3 μm
Positional accuracy	2.5 arc sec
Repeat positioning accuracy	1.0 arc sec
Radial stiffness	1000 N / μm
Axial stiffness	1000 N / μm
Design speed	1500 r / min

Generally, two radial hydrostatic bearings are present in a hydrostatic spindle. Then, the spindle can achieve a higher radial stiffness and has a better resistance to overturning moment. At the same time, it causes a great difficulty for the processing and assembling of a hydrostatic bearing. During the assembling and debugging, it was difficult to measure the alignment of two bearings. An electric spindle should have a compact structure and high precision. Therefore, a new type of hydrostatic bearing support was designed in this study as shown in Fig. 5. To improve the machining accuracy and reduce the processing difficulty, a split design was used in the bearing rotating part, and the three parts were assembled using a screw. This improved the rotation accuracy of bearing.

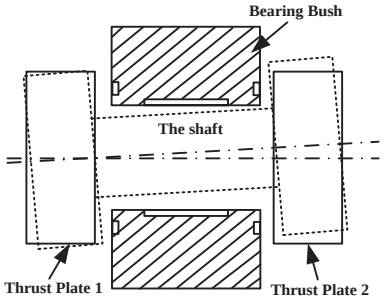

Fig. 5. Practical support form of the bearing

The annular slot choke shown in Fig. 6 was used in the hydrostatic bearing, where hc is the throttle clearance, and lc is the throttle length. The annular slot choke has the advantages of a compact structure, easy to assemble and disassemble, and difficult to block. Thus, the long-term stable operation of the hydrostatic bearings with oil was ensured.

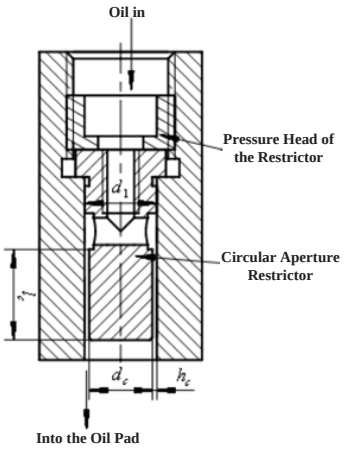

Fig. 6. Circular aperture restrictor

The shape and size of the motor affect the structure design. In this study, the inner rotor torque motor of Kollmorgen company was used. A Kollmorgen frame torque motor is divided into KBM and KBMS types. Compared to the KBM-type torque motor, the KBMS-type torque motor has a Holzer effect sensor that can achieve the locking-type digital control of the motor after the precalibration.

Rotary encoder is an important sensing element for the angle measurement; it is used to convert the angular displacement into an electric pulse signal. The series production of contactless-type circular grating of Renishaw company was selected; it can eliminate the mechanical hysteresis, thus lacking backlash and improving the repeatability. Its fine pitch provides excellent positional stability, achieves a smoother speed control and precise small amplitude incremental movement with extremely low electronic subdivision error of the Sigmund subdivision control.

An oil pump was installed on the hydraulic pressure pump station. The lubricating oil was pumped into a water cooling machine for cooling, thus maintaining the lubricating oil temperature in the hydraulic station in a stable range. A pneumatic seal was used between the two rotary members in the spindle, and the pressure was 2–3 bar. Therefore, a dynamic seal of the lubricating oil was obtained, and the spindle work environment provided precision machining.

The work of hydrostatic bearing relied on the oil supply of the external hydraulic station. The design of a hydraulic station should satisfy the following basic requirements: (1)

Oil pressure and oil flow should be designed to satisfy the requirements of a hydrostatic bearing. (2) The oil should be clean. The oil film clearance of a hydrostatic bearing is 20 μm, and the restriction gap of the chock is 20 ~ 40 μm. Therefore, if the oil contains impurities, the chock may block, thus affecting the normal operation of the hydrostatic bearing. (3) An oil supply system should have a safety device; in the case of a power failure, the hydraulic system should supply the oil. Therefore, a bladder-type accumulator is generally installed in the hydraulic system. (4) An adequate heat dissipation area or a temperature adjustment device should be present.

When the oil temperature increases, the lubricating oil viscosity decreases. Usually the oil is pumped using a hydraulic pump to an oil or water cooler and uses a temperature sensor to monitor the temperature of the lubricating oil. When the temperature reaches the limit, the oil or water cooler starts to work and cools the lubricant. The hydraulic system of the hydrostatic bearing is shown in Fig. 7.

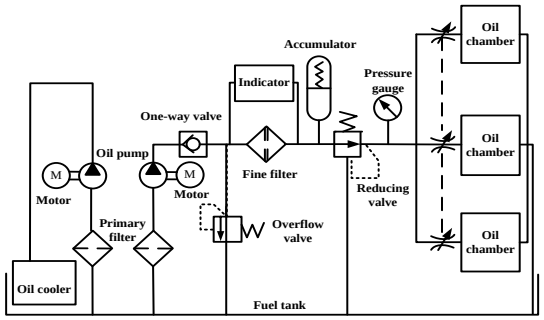

Fig. 7. Principle diagram of thehydrostatic spindle's hydraulic system

A 3D model of the hydrostatic spindle is shown in Fig. 7(a). The test system for the accuracy detection of the spindle is shown in Fig. 7(b). In this system, a TT90 micro displacement meter, boxGT42 inductive measuring instrument, and standard ball were used to spindle radial and axial error measurements.

The radial rotation accuracy and axial motion error of the spindle are shown in Table 12; both of them satisfy the design index of 0.3 μm. Further test results show that other indicators such as positional accuracy, repeat positioning accuracy, radial stiffness, axial stiffness, and speed also satisfy the design requirements.

Table 12. Radial rotation accuracy and axial motion error of the spindle

Serial number in measuring	Radial rotation accuracy (μm)	Axial motion error (μm)
1	0.15	0.07
2	0.29	0.09
3	0.19	0.08

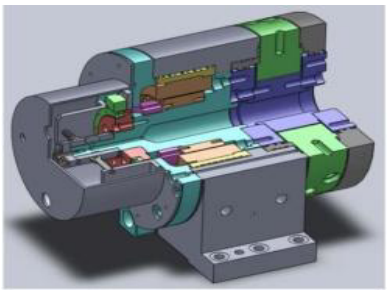

(a)

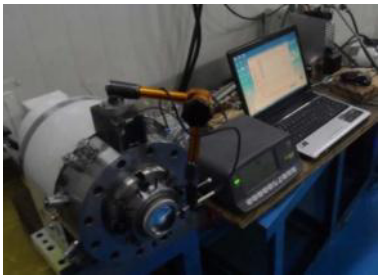

(b)

Fig. 8. (a) 3D model of the hydrostatic spindle; (b) Test system of the hydrostatic spindle

6. Conclusion

(1) Considering the working conditions of a hydrostatic spindle, the principles of the design process are provided in this paper. The design process includes bearings, seals, rotors, strong coupling, tribology, dynamics, fluid mechanics, and multisubject information.

(2) To decouple and integrate all the multisource information, an axiomatic design method for the hydrostatic spindle is proposed. Four levels of FRs and DPs for the spindle design were mapped.

(3) A design flow chart of the hydrostatic spindle was obtained based on the multisource information, and a spindle design was guided by this process.

Acknowledgments

This work was supported by the National Natural Science Foundation of China (NSFC51275395) and National Science and Technology Major Project of the Ministry of Science and Technology of China (2012ZX04002-091).

References

[1] Chen Yanlin, duanZhilin, XIONG Wanli. Research status and development of high speed motorized spindle. Mechanical RESEARCH&Application, 2004, 17(4):10-11.

[2] XIONG Wanli, YANG Xuebing, LV Lang et.al. Review on Key Technology of Hydrodynamic and HydrostaticHigh-frequency Motor Spindles. Journalof Mechanical Engineering, 2009, 45(09):1-18.

[3] Du Xiong. Design of embedded static electric spindle shaft system. Precise Manufacturing & Automation,2013(3):26-29.
[4] WU Liangsheng, ZHOU Liang, XIAO Yichuan. Dynamic Performance for GDH512 Motorized Spindle. Manufacturing Technology&Machine Tool, 2010(2):21-25.
[5] ZHONG Xianxin. High accuracy of precision spindle system. Precise Manufacturing & Automation, 1987(2).
[6] WANG Bo, SUN Wei, WEN Bangchuan. The Effectof High Speedson Dynamic Characteristics of Motorized Spindle System. EngineeringMechanics, 2015(6):231-237.
[7] MU Yang, LUO Ping, LIU Heng et.al.Stability Analysis and Experiment for Electric Spindle of Turning-milling MC.Modular Machine Tool&Automatic Manufacturing Technique, 2011(3):4-7.
[8] SUH N P. Axiomatic design: Advances and applications. New York: Oxford University Press, 2001.
[9] XIE Youbai, YUAN Xiaoyang,XU Hua et.al. Axiomaticdesign: Advances and applications. Beijing:ChinaMechanical Press, 2004.
[10] ZHANG Libin, SHI Weimin, BAO Guanjun, et.al.General design process model based on axiomaticdesign. Journal of Mechanical Engineering, 2010, 46(23): 166-173.
[11] Stephen C Y Lu, Nam-Pyo Suh.Complexity in design of technical systems.Manufacturing Technology, 2009, 58(1): 157-160.
[12] Nam-Pyo Suh.Complexity in Engineering.Manufacturing Technology, 2005, 54(2):46-63.
[13] XIAO Renbin, CHENG Xianfu, CHEN Cheng, et.al. New approach to product platform design based on axiomatic esign and design relationship matrix. Journal of Mechanical Engineering,2012,48(11):94-103.
[14] LIU Xize,QI Guoning,JI Yangjian,et.al. Productplatform design method based on complex network andaxiomatic design. Journal of Mechanical Engineering,2012,48(11):6-93.
[15] Ananthkrishnan N. Conceptual Design of an Aerospace Vehicle Controller Using Axiomatic Theory. Journal of Aircraft, 2010, 47(6):2149-2151.
[16] JIA Qian, LI Yuezong, CHEN Runlin,et al. Forming Process of Bearing Materials suitable for High-speed Bearing. China Mechanical Engineering, 2014(21): 2860-2864.